



The role of SerpinB2 in human bronchial epithelial cells responses to particulate matter exposure

Eleonora Longhin¹ · Marina Camatini¹ · Audun Bersaas² · Paride Mantecca¹ · Steen Mollerup²

Received: 19 March 2018 / Accepted: 4 July 2018 / Published online: 9 July 2018
© Springer-Verlag GmbH Germany, part of Springer Nature 2018

Abstract

Exposure to particulate matter (PM) has been related to the onset of adverse health effects including lung cancer, but the underlying molecular mechanisms are still under investigation. Epithelial-to-mesenchymal transition (EMT) is regarded as a crucial step in cancer progression. In a previous study, we reported EMT-related responses in the human bronchial epithelial cell line HBEC3-KT, exposed to Milan airborne winter PM_{2.5}. We also found a strong modulation of *SERPINB2*, encoding for the PAI-2 protein and previously suggested to play an important role in cancer. Here we investigate the role of *SERPINB2*/PAI-2 in the regulation of EMT-related effects induced by PM exposure in HBEC3-KT. PM exposure (up to 10 µg/cm²) increased *SERPINB2* expression, reduced cell migration and induced morphological alterations in HBEC3-KT. Changes in actin structure and cadherin-1 relocalization were observed in PM-exposed samples. Knockdown of *SERPINB2* by siRNA down-regulated the *CDH1* gene expression, as well as PAI-2 and cadherin-1 protein expression. *SERPINB2* knockdown also increased cell migration rate, and counteracted the PM-induced reduction of cell migration and alteration of cell morphology. *SERPINB2* was found to be greatly down-regulated in a HBEC2-KT transformed cell line, supporting the importance of this gene in the regulation of EMT. In conclusion, here we show that PAI-2 regulates *CDH1* gene/cadherin-1 protein expression in bronchial HBEC3-KT cells, and this mechanism might be involved in the regulation of cell migration. *SERPINB2* down-regulation should be considered part of EMT, and the over-expression of *SERPINB2* in PM-exposed samples might be interpreted as an initial protective mechanism.

Keywords *SERPINB2* · PAI-2 · Epithelial to mesenchymal transition · Particulate matter · Cell migration · Cadherin-1

Background

Exposure to particulate matter (PM) has been related to the onset of adverse health outcomes, including pulmonary and cardiovascular diseases, and lung cancer (Lewtas 2007),

but the molecular mechanisms underlying the development of these diseases are still under investigation. With regard to lung cancer, PM is suggested to function as an initiator in the carcinogenic process because of its DNA-damaging potential, leading to oxidative damage and the formation of bulky adducts (Valavanidis et al. 2013; Cassee et al. 2013). Besides, chemical compounds in the particles, such as PAHs, are known to be complete carcinogens, contributing to cancer promotion and progression by affecting physiological processes that modulate cell growth, division, proliferation (Liu et al. 2015). Epithelial-to-mesenchymal transition (EMT) is regarded as a crucial step in cancer progression (Xiao and He 2010a). This process involves morphological and phenotypic cellular changes, including loss of cell–cell adhesion, polarized epithelial morphology, and acquisition of a motile and invasive phenotype. The most typical molecular changes include loss of cell–cell adhesion protein cadherin-1 (*CDH1* gene) expression, and enhanced cadherin-2

Electronic supplementary material The online version of this article (<https://doi.org/10.1007/s00204-018-2259-z>) contains supplementary material, which is available to authorized users.

✉ Eleonora Longhin
eleonora.longhin@unimib.it

✉ Paride Mantecca
paride.mantecca@unimib.it

¹ Department of Earth and Environmental Sciences, Polaris Research Centre, University of Milano-Bicocca, Piazza della Scienza, 1, 20126 Milan, Italy

² Department of Biological and Chemical Working Environment, National Institute of Occupational Health, 0033 Oslo, Norway

(*CDH2* gene) and intermediate filament protein vimentin (*VIM* gene) expression (Xiao and He 2010b).

Several recent *in vitro* studies reported alterations in cell migration and invasion, and in EMT markers expression (Yue et al. 2015; Yang et al. 2017; Wei et al. 2017) and cell transformation after 3 months exposure to PM (Luanpitpong et al. 2014). It has been suggested that the mechanisms underlying these changes involve the extracellular matrix (ECM) degradation pathway (Yue et al. 2015). In lung cancer cells exposed to PM, Yang and colleagues reported the regulation of vimentin and cadherin-1, involved in mechanisms regulating cell–cell adhesions, mobility and proliferation of epithelial cells (Yang et al. 2017). In this case, metals in particles were held responsible for this effect. The mechanisms involved in PM-induced EMT are likely to be multiple and diverse according to the chemical composition and properties of particles.

Using HBEC3-KT cells, we previously reported that a low dose (2.5 $\mu\text{g}/\text{cm}^2$) of Milan airborne winter PM_{2.5} (wPM_{2.5}) is capable of inducing EMT-related effects (Longhin et al. 2016b), such as reduced migration and morphological changes starting from 72 h of exposure, and reduced cadherin-1 expression after 2 weeks of exposure. HBEC3-KT may constitute a suitable model for studying molecular carcinogenic pathways in normal lung cells. HBEC3-KT has been immortalized from normal bronchial epithelium in the absence of viral oncoproteins, by stable transfection of the *hTERT* and *Cdk4* genes. HBEC3-KT do not generate colonies in soft agar or tumors in nude mice, retain an intact TP53 signaling pathway, and their gene expression pattern clusters with normal non-immortalized bronchial epithelial cells and not with lung tumor cells (Ramirez et al. 2004).

The alterations on migration and morphology induced by particles exposure on HBEC3-KT were compared with modulation of genes that are relevant for several biological processes, including response to xenobiotics and oxidative stress, inflammatory processes and EMT (Longhin et al. 2016b). Among the affected genes we found a strong and early up-regulation of *SERPINB2*, coding for the plasminogen activator inhibitor type-2 protein PAI-2. The role of this serpin has long been enigmatic, but it has been previously suggested to play an important role in cancer (Croucher et al. 2008). High levels of PAI-2 have been related to inhibition of metastasis in mice (Schroder et al. 2014), while low expression was associated with reduced survival from lung adenocarcinoma in humans (Ramnefjell et al. 2017). *In vitro*, PAI-2 has been reported to inhibit proliferation and migration in pulmonary arterial smooth muscle cells (Zhang et al. 2015). The mechanisms of these effects are not yet fully elucidated. In the extracellular environment, serpins inhibit the urokinase plasminogen activator (uPA), preventing the conversion of plasminogen to plasmin, which participates in the breakdown and remodelling of the ECM, facilitating

invasion and metastasis. This function has primarily been attributed to serpinE1 (PAI-1), PAI-2 being approximately tenfold slower than PAI-1 at inhibiting uPA, and is usually not detectable in human plasma under physiological conditions (Croucher et al. 2008). Thus, other mechanisms might link PAI-2 to cell proliferation and migration. Taking into account the prevalence of the cytosolic form of this protein over the released form, intracellular functions have been suggested. However, due to conflicting results and specific responses in different cell types, the exact function of intracellular PAI-2 remains unclear (Croucher et al. 2008).

We hypothesized that *SERPINB2*/PAI-2 may play a role in the regulation of migration induced by PM exposure in HBEC3-KT, and possibly in other EMT-related effects. To test this hypothesis, we further exposed these cells to Milan PM and we used small interfering RNA (siRNA) for *SERPINB2* gene expression knockdown. Cell migration and morphology, and the expression of EMT-related genes and proteins were thus assessed.

Methods

PM sampling and preparation for biological experiments

PM_{2.5} samples were collected during winter 2011–2012 at Torre Sarca, a site of urban background for atmospheric pollution in Milan. Samplings were performed by a low volume gravimetric sampler (FAI Instruments, Rome, Italy) on Teflon filters, which were replaced every 24 h and then stored at $-20\text{ }^\circ\text{C}$ until extraction. Samples were pooled and particles were extracted as previously described (Longhin et al. 2013). Briefly, filters were put in a glass vial with 2 mL of sterile water and underwent 20 min sonication in an ultrasound bath (SONICA, Soltec). Four sonication cycles were performed and the extraction water was collected and replaced every time. The volumes obtained from the four cycles were put together to obtain a homogeneous sample. Particle suspension was aliquoted in sterile vials, dried in a desiccator, weighed and stored at $-20\text{ }^\circ\text{C}$. The resulting pellets were resuspended in sterile water (2 $\mu\text{g}/\mu\text{L}$) just prior to use.

Data on the PM chemical composition and physical properties have been published previously (Mantecca et al. 2012).

Cells culture and exposure

The *hTERT* and *Cdk4* immortalized human bronchial epithelial cell lines HBEC3-KT and HBEC2-KT were a kind gift from Dr. John D. Minna (Ramirez et al. 2004). During a previous study, transformed cell lines were established from HBEC2-KT after long-term exposure to a cigarette smoke

condensate (Bersaas et al. 2016). The cell line code T2KT-CSC-H, referred to as transformed HBEC2-KT, was used in this study.

Cells were maintained on collagen-coated dishes in LHC-9 medium at 37 °C with 5% of CO₂. For the maintenance of transformed HBEC2-KT, 10% FBS was added to the medium.

HBEC3-KT cells were used for PM exposure and knock-down experiments. They were seeded at a concentration of 3×10^5 cells/well in 6-well plates and treated the day after with 2.5 or 10 µg/cm² of wPM2.5. The cellular responses were examined after 6, 24, 48 and 72 h of exposure and the results compared to untreated cells (control).

HBEC2-KT and transformed cells were used to investigate *SERPINB2* gene expression levels in cells that already underwent the EMT process versus normal cells.

RNA interference

HBEC3-KT cells for RNA interference were seeded at a concentration of 2×10^5 cells/well in 6-well plates. After 24 h, the cells were incubated with LHC-9 plus transfection media (4:1), containing a combination of three different *SERPINB2* specific siRNAs (1:1:1 of HSS107572, HSS107573, HSS107574, Thermo Fisher, final concentration 5 nM; sequences are reported in Additional file 1) or negative control siRNA (Stealth RNAi Negative Control Medium GC Duplex, Thermo Fisher, final concentration 5 nM), according to the manufacturer's forward transfection protocol. Transfection media were prepared by diluting lipofectamine RNAiMAX (Thermo Fisher) and siRNA (or negative control siRNA) in Opti-MEM reduced serum medium (Thermo Fisher), and incubated at room temperature for 5 min prior to transfection.

After 24 h of incubation, transfection media were removed and cells were exposed to 10 µg/cm² of wPM2.5 for 48 h. The PM concentration and time point were selected after screening of the effects induced at the screening conditions described in paragraph 2.2. The cells were then used for the different biological analyses as described below.

For migration assays on *SERPINB2* knockdown studies, a reverse transfection protocol was used. After trypsinization, the cells were directly resuspended in LHC-9 plus transfection media and seeded (2.5×10^4 cells/well) in a collagen-coated ImageLock 96-well plate (Essen Bioscience), so that seeding and transfection occurred at the same time for 24 h. Then the cells were exposed to 10 µg/cm² of wPM2.5 for 48 h, and the scratch wound was performed.

Gene expression

Total RNA was extracted from samples by the RNA-Solv Reagent (Omega Bio-tek) and reverse transcribed using

qScript cDNA Synthesis kit (Quanta Biosciences). Measurement of gene expression was performed by real-time PCR on a StepOne Plus Real-Time PCR system (Applied Biosystems), using the PerfeCTa SYBR Green FastMix (Quanta Biosciences) and the following program: initial denaturation at 95 °C for 30 s, then 40 cycles of 95 °C for 3 s and 60 °C for 30 s, followed by a melting curve. The amount of target cDNA in each sample was established by determining a fractional PCR threshold cycle number (Ct), and estimated by interpolation from a standard curve. The standard curve was made from known amounts of the corresponding product with the same primer sets and was run on each PCR plate. The expression levels of target genes were normalized to the expression of 18S. Primers sequences for investigated genes *SERPINB2*, *CDH1*, *VIM* and 18S are reported in Additional file 2.

Cell migration

A scratch wound closure assay was used for migration analysis. For the experiments involving PM exposure (Fig. 1b), cells were seeded (2×10^4 cells/well) in a collagen-coated ImageLock 96-well plate (Essen Bioscience). After 24 h, cells were exposed to PM for 48 h. Scratch wound was performed by use of the WoundMaker tool (Essen BioScience) and migration was followed for 24 h and determined by an InCuCyte Zoom Live Cell Imaging microscope and associated software (Essen BioScience).

For migration experiments involving *SERPINB2* knock-down (Fig. 4), the seeding and transfection steps were performed simultaneously for 24 h, as described in paragraph 2.3.

Cell morphology and immunocytochemistry

Cell morphology was inspected after PM exposure by a Nikon ECLIPSE TS100 inverted microscope, and digital images were acquired. Cells for immunocytochemical detection of proteins were prepared following common fluorescence microscopy techniques. Briefly, cells were grown on cover slips and treated as described above. After exposure, cells were washed in PBS and fixed with 4% paraformaldehyde for 15 min at 4 °C. Permeabilization and blocking were performed in PBS, 5% BSA, 0.1% Triton X-100 for 60 min at room temperature. Cells were then immunocytochemically labelled with primary antibodies in PBS, 3% BSA overnight at 4 °C (cadherin-1 1:300 dilution; vimentin 1:150; PAI-2 1:500; Thermo Fisher). Cover slips were then incubated with appropriate Alexafluor 488 secondary antibodies (1:500 dilution; Thermo Fisher) for 1 h at room temperature. Actin was labelled with rhodamine phalloidin (1:40 dilution, Thermo Fisher) in PBS/1% BSA for 20 min at room temperature. Slides were mounted with ProLong Gold

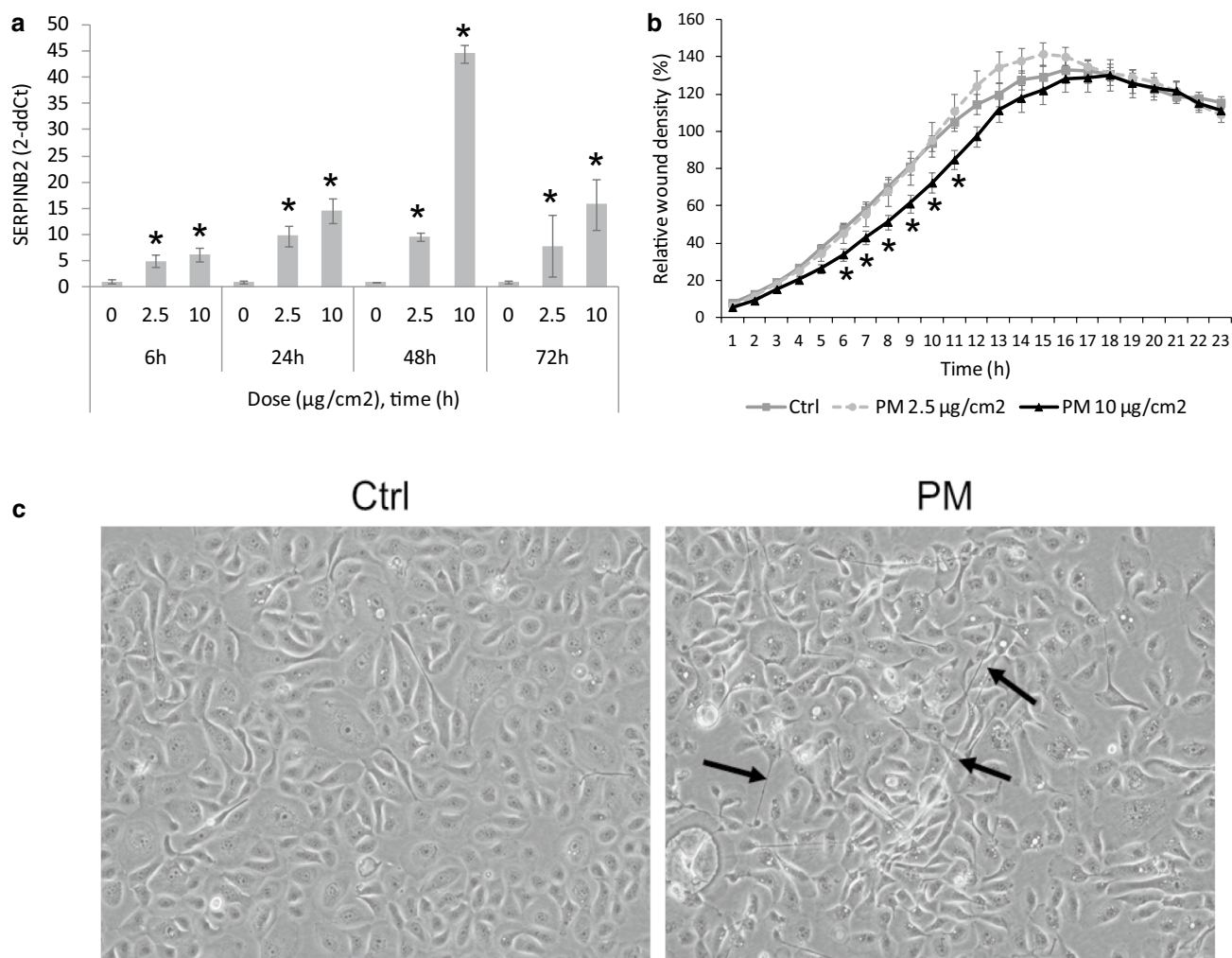


Fig. 1 PM effects on HBEC3-KT cells. **a** *SERPINB2* expression was measured after exposure to 2.5 and 10 µg/cm² of PM, from 6 to 72 h. *Statistically significant difference from untreated cells (Ctrl), *t* test $p < 0.05$. **b** Effects on migration were investigated after 48 h of PM exposure. *Statistically significant difference from untreated cells

(Ctrl), linear mixed model $p < 0.05$. **c** Morphological alterations regarding increased presence of elongated spindle-like cellular structures (arrows), were observed after 48 h of exposure to 10 µg/cm² of PM

antifade reagent (Thermo Fisher), which included DAPI for the cell DNA counterstaining. Slides were observed under the inverted microscope AxioObserver Z1 Cell Imaging station (Carl-Zeiss Spa, Germany) and images were acquired by a MRc5 digital camera and elaborated with the dedicated software AxioVision Rel. 4.8.

Western blotting

Cells were scraped and lysed on ice with sample buffer (60 mM Tris pH 6.8, 1.5% SDS, protease inhibitors, 12.5 mM DTT added to the cell solution). The total protein content was evaluated by the bicinchoninic acid assay (Thermo Fisher) according to the manufacturer's instruction. Equal amounts of proteins were loaded onto precast

Mini-PROTEAN Stain-Free Protein Gels (Bio-Rad), separated and transferred onto nitrocellulose membranes. Actin staining was used for assessment of equal protein loading. The membranes were then blocked overnight (Tris buffered saline, TBS, 0.2% Tween20, 3% (w/v) Bovine Serum Albumin, BSA) and incubated at 4 °C overnight with specific primary antibody diluted according to data-sheets (PAI-2 dil. 1:3000, cadherin-1 dil. 1:10,000, β-actin dil. 1:10,000, Thermo Fisher). The day after, membranes were washed in TBS and incubated with specific HRP-linked secondary antibodies for 1 h at RT (anti-rabbit or mouse IgG, 1:10,000, Cell Signaling). After detection with chemiluminescent peroxidase substrate (Thermo Fisher), digital images were taken by a luminescence reader (Amersham Imager 600) and densitometry analysis

performed with dedicated software (Amersham Imager 600 Analysis Software Version 1.0).

Statistical analyses

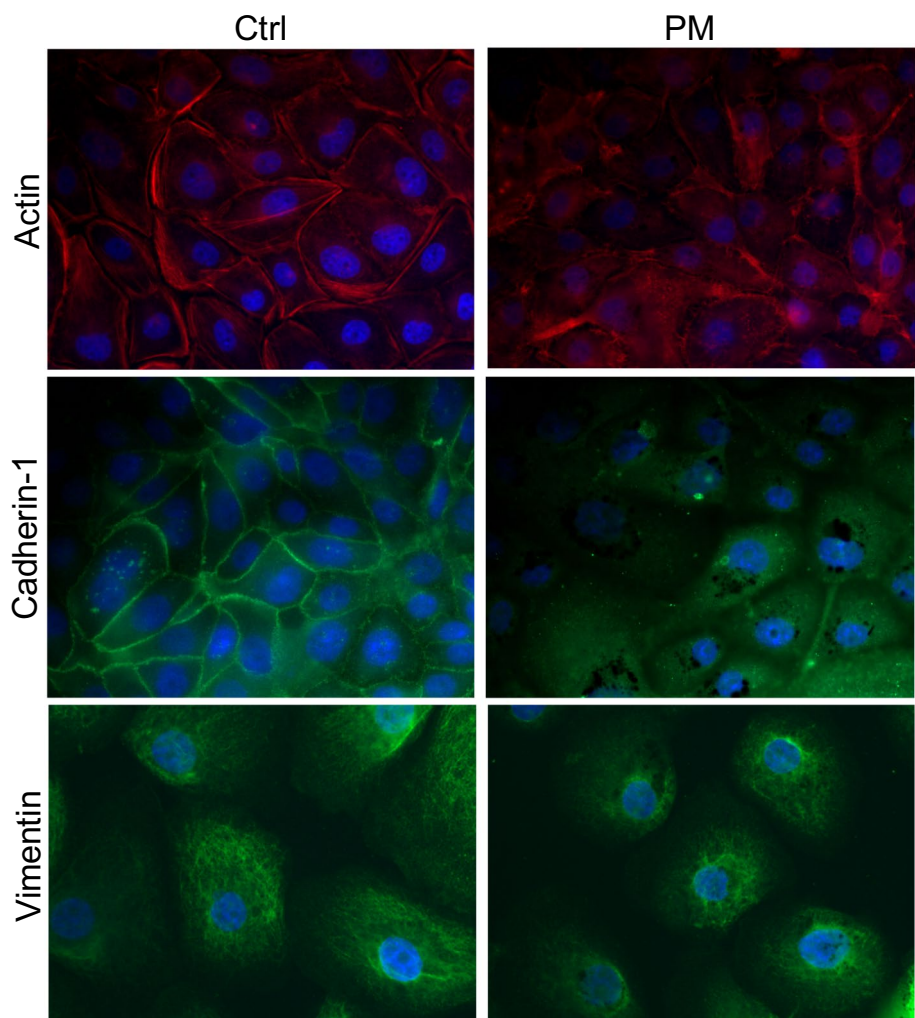
Mean and standard deviation (SD) of at least three independent experiments are reported. Statistical analyses were performed by Sigma Stat 3.1 software, using *t* test. Values of $p < 0.05$ were considered statistically significant. Cell migration was analyzed by a linear mixed model (Stata, Stata-Corp LP). An interaction term between treatment and time allowed us to estimate the difference over time between the transformed cell lines and the control cell line. To take into account the dependency in the data, random effects were added for wells, while a random slope for time accounted for different individual slopes of the curve for each well. Finally, an autoregressive (AR) structure of order 2 was assumed for the residuals.

Results

We have previously reported reduced migration and altered morphology starting from 72 h of exposure, and reduced cadherin-1 expression after 2 weeks of exposure to a low dose ($2.5 \mu\text{g}/\text{cm}^2$) of Milan wPM2.5 (Longhin et al. 2016b). A time course and dose response screening was performed on *SERPINB2* expression in HBEC3-KT cells exposed to PM to select optimal conditions for the siRNA studies. The strongest induction was detected after 48 h of exposure to the dose $10 \mu\text{g}/\text{cm}^2$ (Fig. 1a). At this exposure condition, migration of cells was reduced (Fig. 1b) and morphology was altered, with higher presence of elongated spindle-like structures (Fig. 1c, arrows).

Morphological alterations were further investigated by fluorescence microscopy, by marking the cytoskeletal proteins actin and vimentin, and the membrane cell–cell adhesion protein cadherin-1. Alteration in actin structure, consisting in loss of stress fibers and increased membrane

Fig. 2 Actin, cadherin-1 and vimentin analyses by immunocytochemistry. Cells were exposed for 48 h to $10 \mu\text{g}/\text{cm}^2$ of PM and stained for actin (red), cadherin-1 or vimentin (green), and DNA (blue)



ruffling, was observed (Fig. 2), as previously reported in BEAS-2B cells exposed to Milan winter PM_{2.5} (Longhin et al. 2016a). As expected, cadherin-1 localized at junctions between adjacent cells in control samples, while a less specific and more diffuse staining was observed in the cytoplasm of PM-exposed cells (Fig. 2). Less distinct alterations in vimentin were observed.

To investigate the role of PAI-2 on migration and other EMT markers, knockdown experiments with *SERPINB2* siRNA were carried out. At the time point studied, the down-regulation of *SERPINB2* was highly effective (Fig. 3). Negative siRNA control (siNEG) did not affect *SERPINB2* levels with respect to control cells or PM-exposed samples (Ctrl and PM).

The expression of EMT-related genes *CDH1*, *CDH2* and *VIM* was thus measured. PM exposure did not significantly affect the expression of these genes at the time point investigated. Very interestingly, *SERPINB2* knockdown statistically significantly down-regulated *CDH1* expression; fold change in not exposed and PM-exposed samples was reduced by 87 and 85%, respectively, compared to siNEG control cells. No significant effects were observed on the other genes here investigated (Fig. 3).

SERPINB2 knockdown induced increased cell migration rate in HBEC3-KT cells, while transfection with siNEG had no effect (Fig. 4a). Moreover, knockdown of *SERPINB2* partly counteracted the PM-induced reduction of cell migration (Fig. 4b).

Knockdown of *SERPINB2* also inhibited the PM-induced alterations of cell morphology, reducing the presence of elongated spindle-like structures (Fig. 5). Negative siRNA control did not alter PM-induced effects on morphology.

Fluorescence microscopy was again used to investigate the effect of *SERPINB2* knockdown on proteins of interest. Cadherin-1 was marked to assess the effect of *CDH1* down-regulation at protein level, while actin was marked to investigate possible effects on the morphological alteration observed after PM exposure. Cadherin-1 relocalization after PM exposure was confirmed in cells treated with negative siRNA control (Fig. 6). Cadherin-1 fluorescence intensity was greatly reduced in samples in which *SERPINB2* was knocked down, supporting *CDH1* down-regulation. Alterations of actin induced by PM did not appear to be affected by *SERPINB2* knockdown, as membrane ruffling and loss of stress fibers were still evident in these cells (Fig. 6).

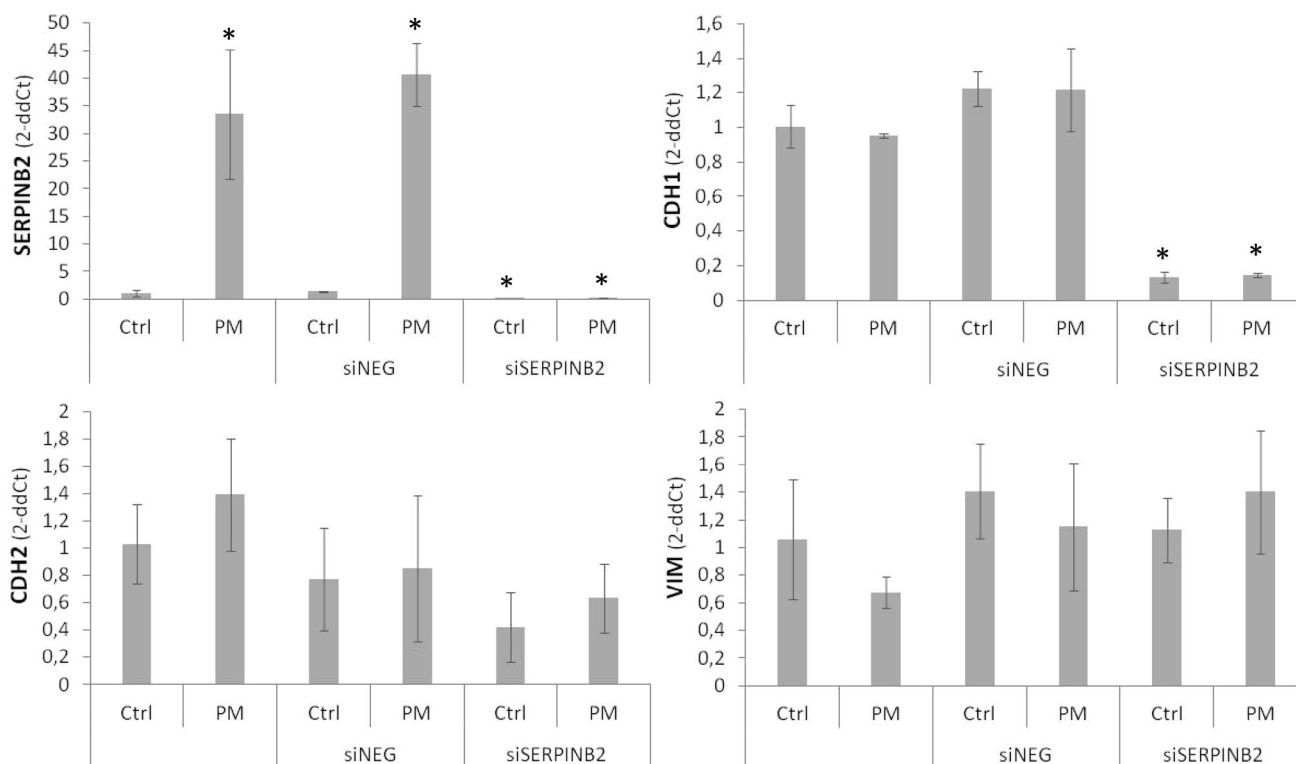


Fig. 3 Gene expression analysis after *SERPINB2* knockdown. Cells were incubated for 24 h with siRNA against *SERPINB2* (siSERPINB2) or negative siRNA control (siNEG), and then exposed for

48 h to 10 $\mu\text{g}/\text{cm}^2$ of PM. *Statistically significant difference from untreated cells (Ctrl), *t* test $p < 0.05$

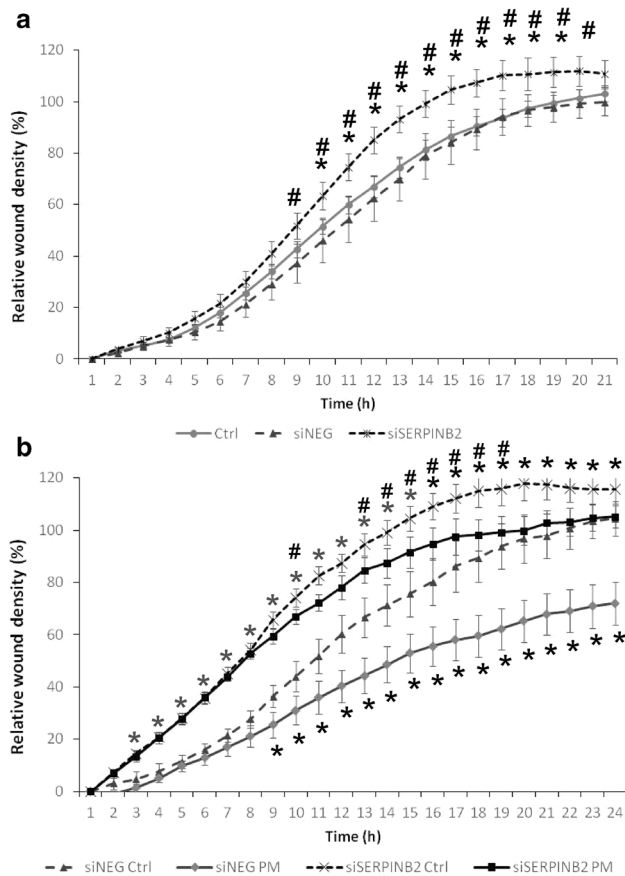


Fig. 4 Analysis of cell migration after *SERPINB2* knockdown. **a** Cells were seeded, and after 24 h, incubated for additional 24 h with siRNA against *SERPINB2* (siSERPINB2), negative siRNA control (siNEG), or fresh medium (Ctrl). Scratch wound healing assay was then carried out. Statistically significant difference from * untreated cells (Ctrl), # negative siRNA control (siNEG), linear mixed model $p < 0.05$. **b** Cells were seeded and simultaneously incubated with siRNA against *SERPINB2* (siSERPINB2) or negative siRNA control (siNEG) for 24 h, and then exposed for 48 h to $10 \mu\text{g}/\text{cm}^2$ of PM. Scratch wound healing assay was then run. *Statistically significant difference from siNEG Ctrl (gray asterisks refer both to siSERPINB2 Ctrl and siSERPINB2 PM), #Statistically significant difference of siSERPINB2 PM from siSERPINB2 Ctrl. Linear mixed model $p < 0.05$

Effects of *SERPINB2* knockdown on PAI-2 and cadherin-1 proteins were confirmed by Western blotting (Fig. 7). As expected, PAI-2 was induced by PM, and expression was almost completely abrogated after *SERPINB2* knockdown. Small alterations in actin protein levels may be apparent in PM-exposed cells (Fig. 7).

Finally, as a further indication of the importance of *SERPINB2* in the regulation of EMT, we measured its expression in a previously established in vitro transformed cell line (transformed HBEC2-KT). Very interestingly,

SERPINB2 is greatly and statistically significantly down-regulated in the transformed cell line, compared to the original untransformed HBEC2-KT (Fig. 8). The expression of EMT-related genes *CDH1*, *CDH2* and *VIM* was here measured and reported to confirm the maintenance of the typical gene expression pattern of transformed cell lines that have gone through EMT. As expected, *CDH1* down-regulation, and *CDH2* and *VIM* up-regulation were present (Fig. 8).

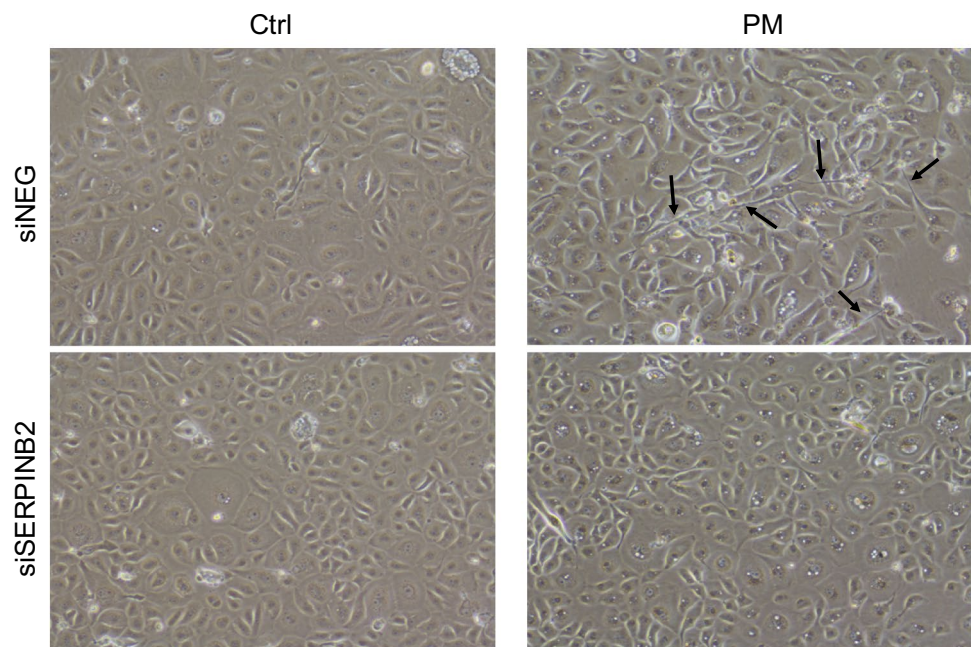
Discussion

PM exposure has been related to lung cancer and development of EMT, but the mechanisms underlying these outcomes are still poorly understood. The primary aim of this work was to investigate the importance of *SERPINB2*/PAI-2 in the EMT process induced by PM exposure in HBEC-3KT cells. Previously, we reported that diesel exhaust particles and winter Milan PM_{2.5} induce *SERPINB2* expression and delayed migration in this cell model (Longhin et al. 2016b). Moreover, high PAI-2 levels have been related to reduced migration of pulmonary arterial smooth muscle cells in vitro, while knockdown of PAI-2 has been shown to increase proliferation and migration (Zhang et al. 2015). Here we confirm these observations in a normal bronchial epithelial cell line (HBEC3-KT), showing that knockdown of *SERPINB2* induces increased cell migration rates in control and PM-exposed cells, counteracting the delayed migration induced by PM.

To investigate the mechanisms of the observed correlation between *SERPINB2* and migration, we analyzed other EMT markers and possibly related effects. Although increased migration is a typical hallmark of EMT, decreased or delayed cell migration has also been described in post-EMT human epithelial cells (Schaeffer et al. 2014). The same effect was reported in murine lung epithelial cells exposed to diesel particles (LaGier et al. 2013). In this last case, the authors found decreased cytoskeletal anchoring, along with altered Golgi polarity, modified focal adhesions, and thus relating the delay in cell migration to these cytoskeletal alterations.

Interestingly, PM exposure resulted in altered cell morphology, with an increased number of elongated spindle-like structures, modified actin structure, loss of stress fibers and increased membrane ruffling. In addition, Cadherin-1 was found to relocalize after PM exposure, moving from the cell–cell contact region to the cell’s cytoplasm. A few papers reported similar effects in PM-exposed cells. Actin alterations were reported in A549 cells exposed to PM₁₀, although in this case stress fibers were increased

Fig. 5 Cell morphology after *SERPINB2* knockdown. Cells were incubated for 24 h with siRNA against *SERPINB2* (siSERPINB2) or negative siRNA control (siNEG), and then exposed for 48 h to 10 $\mu\text{g}/\text{cm}^2$ of PM. Arrows indicate elongated spindle-like cellular structures



after particle exposure (Chirino et al. 2017). In HUVECs exposed to diesel particles, Tseng et al. (2015) reported vascular endothelial (VE)-cadherin relocation, moving from the cell membrane to the interior and intracellular submembrane regions, though maintaining unaffected protein levels.

Brandhagen et al. (2013) reported similar morphological changes in cell morphology, including loss of cortical actin and stress fibers, and gain of peripheral membrane ruffles in SKOV-3 ovarian carcinoma cells exposed to the synthetic steroid mifepristone. These alterations of the overall architecture of the cytoskeleton were associated with poor cell adhesion (Brandhagen et al. 2013) and might be partly responsible of the reduced migration in PM-exposed cells. In particular, a high frequency of ruffle formation has been associated with inefficient cell adhesion and migration (Borm et al. 2005).

Knockdown of *SERPINB2*/PAI-2 resulted in increased migration rate. However, it did not appear to have any effect on PM-induced structural modification of actin, since loss of stress fibers and increased membrane ruffles are still evident in PM-exposed samples. Nevertheless, the cell morphology appeared to be affected, since the elongated spindle-like structures present in PM-exposed samples were almost completely absent after PAI-2 knockdown. To our knowledge, this is the first study to report effects of PAI-2 on cell morphology.

Interestingly, PAI-2 knockdown greatly reduced the expression of cadherin-1 at the gene and protein level.

Cadherin-1 is a relevant cell–cell adhesion protein that plays a key role in establishing adherens junctions. Loss of cadherin-1 is a hallmark of EMT, and it has been previously correlated with increased cell migration, through the WT1 pathway (Wu et al. 2013). Loss of cadherin-1 is likely a mechanism linking PAI-2 down-regulation to increased cell migration in our model. On the contrary, the role of cadherin-1 in reduced migration after exposure to PM is less clear. PM exposure induced cadherin-1 relocalization from the membrane to the cytosol, without significantly altering the protein level. In addition to down-regulation of cadherin-1 expression, deregulation of exocytic and endocytic pathways has been reported, with consequences for protein turnover, recycling, sequestration, and degradation (Melo et al. 2017). For example, abnormal activation of proto-oncogenes such as EGFR, c-Met, and Src results in increased phosphorylation of tyrosine residues in the cadherin-1/catenin complex, which leads to protein internalization (Melo et al. 2017). In addition, constitutive activation of Arf6, which is involved in protein trafficking, endocytic recycling and cytoskeleton remodelling, was found to lead to cadherin-1 cytoplasmic accumulation (Figueiredo et al. 2011). Cadherin-1 is known to interact with actin filaments, as well as other cytoskeleton structures (Izaguirre and Casco 2016). The effects of cadherin-1 relocation and actin alterations induced by PM might thus be correlated, but this hypothesis needs further investigations.

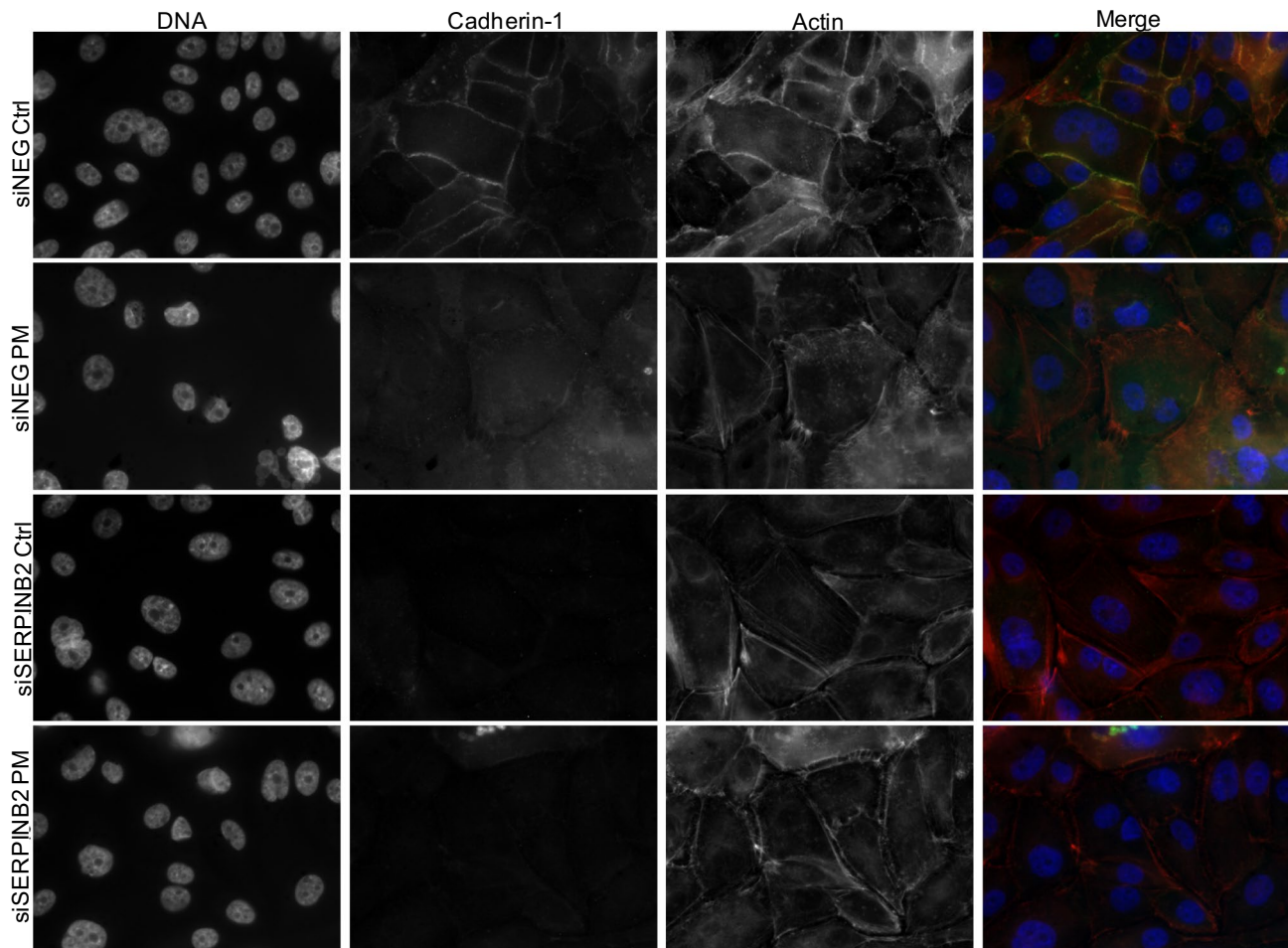


Fig. 6 Actin and cadherin-1 analyses by immunocytochemistry after *SERPINB2* knockdown. Cells were incubated for 24 h with siRNA against *SERPINB2* (siSERPINB2) or negative siRNA control

(siNEG), and then exposed for 48 h to $10 \mu\text{g}/\text{cm}^2$ of PM. Cells were then stained for actin (red), CDH1 (green), and DNA (blue)

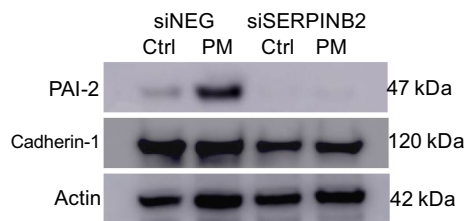
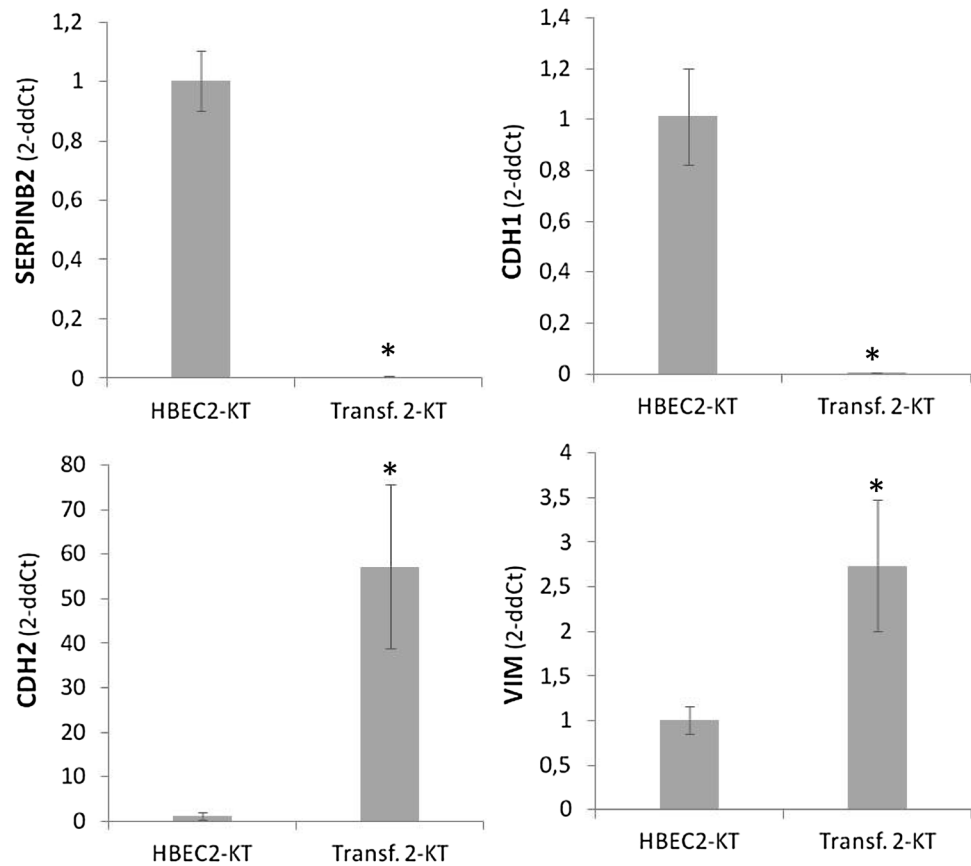


Fig. 7 PAI-2, cadherin-1 and actin protein levels by Western blotting after *SERPINB2* knockdown. Cells were incubated for 24 h with siRNA against *SERPINB2* (siSERPINB2) or negative siRNA control (siNEG), and then exposed for 48 h to $10 \mu\text{g}/\text{cm}^2$ of PM. Images are representative of two independent experiments

To conclude, *SERPINB2*/PAI-2 down-regulation induces increased migration, counteracting the effects of PM exposure. PAI-2 also regulates *CDH1* gene/cadherin-1 protein expression in normal bronchial HBEC3-KT cells, a mechanism that might be involved in the regulation of cell migration. Finally, the observations performed on a transformed cell line suggest that *SERPINB2* down-regulation could be considered part of EMT. In this case, the over-expression of *SERPINB2* in PM-exposed samples might be interpreted as an initial protective mechanism.

Fig. 8 Gene expression analysis in in vitro transformed cells (Transf. 2-KT) compared to the parental cell line (HBEC2-KT). *Statistically significant difference between HBEC2-KT and transformed HBEC2-KT, *t* test $p < 0.05$



Acknowledgements The authors want to thank Øivind Skare for the support with the statistical analyses of the migration data.

Author contributions EL performed the experiments and wrote the manuscript. EL and SM discussed and interpreted the findings. EL, SM and PM designed the project. SM, PM and MC supervised the project and revised the manuscript. AB established the transformed cell line T2KT-CSC-H. All authors have read and approved the final manuscript.

Funding This study has been supported by the grants of the Italian Ministry of Foreign Affairs and International Cooperation (MAECI) to PM (Proj. ID PGR00786).

Compliance with ethical standards

Conflict of interest The authors declare that they have no conflict of interest.

References

- Bersaas A, Arnoldussen YJ, Sjøberg M et al (2016) Epithelial-mesenchymal transition and FOXA genes during tobacco smoke carcinogen induced transformation of human bronchial epithelial cells. *Toxicol In Vitro* 35:55–65. <https://doi.org/10.1016/j.tiv.2016.04.012>
- Borm B, Requardt RP, Herzog V, Kirfel G (2005) Membrane ruffles in cell migration: indicators of inefficient lamellipodia adhesion and compartments of actin filament reorganization. *Exp Cell Res* 302:83–95. <https://doi.org/10.1016/j.yexcr.2004.08.034>
- Brandhagen BN, Tieszen CR, Ulmer TM et al (2013) Cytostasis and morphological changes induced by mifepristone in human metastatic cancer cells involve cytoskeletal filamentous actin reorganization and impairment of cell adhesion dynamics. *BMC Cancer* 13:35. <https://doi.org/10.1186/1471-2407-13-35>
- Cassee FR, Héroux M-E, Gerlofs-Nijland ME, Kelly FJ (2013) Particulate matter beyond mass: recent health evidence on the role of fractions, chemical constituents and sources of emission. *Inhal Toxicol* 25:802–812. <https://doi.org/10.3109/08958378.2013.850127>
- Chirino YI, García-Cuellar CM, García-García C et al (2017) Airborne particulate matter in vitro exposure induces cytoskeleton remodeling through activation of the ROCK-MYPT1-MLC pathway in A549 epithelial lung cells. *Toxicol Lett* 272:29–37. <https://doi.org/10.1016/j.toxlet.2017.03.002>
- Croucher DR, Saunders DN, Lobov S, Ranson M (2008) Revisiting the biological roles of PAI2 (SERPINB2) in cancer. *Nat Rev Cancer* 8:535–545. <https://doi.org/10.1038/nrc2400>
- Figueiredo J, Simões-Correia J, Söderberg O et al (2011) ADP-ribosylation factor 6 mediates E-cadherin recovery by chemical chaperones. *PLoS One* 6:e23188. <https://doi.org/10.1371/journal.pone.0023188>
- Izaguirre MF, Casco VH (2016) E-cadherin roles in animal biology: A perspective on thyroid hormone-influence. *Cell Commun Signal* 14:27. <https://doi.org/10.1186/s12964-016-0150-1>

- LaGier AJ, Manzo ND, Dye JA (2013) Diesel exhaust particles induce aberrant alveolar epithelial directed cell movement by disruption of polarity mechanisms. *J Toxicol Environ Health A* 76:71–85. <https://doi.org/10.1080/15287394.2013.738169>
- Lewtas J (2007) Air pollution combustion emissions: characterization of causative agents and mechanisms associated with cancer, reproductive, and cardiovascular effects. *Mutat Res* 636:95–133
- Liu Y, Yin T, Feng Y et al (2015) Mammalian models of chemically induced primary malignancies exploitable for imaging-based preclinical theragnostic research. *Quant Imaging Med Surg* 5:708–729
- Longhin E, Holme JA, Gutzkow KB et al (2013) Cell cycle alterations induced by urban PM_{2.5} in bronchial epithelial cells: characterization of the process and possible mechanisms involved. *Part Fibre Toxicol* 10:63
- Longhin E, Capasso L, Battaglia C et al (2016a) Integrative transcriptomic and protein analysis of human bronchial BEAS-2B exposed to seasonal urban particulate matter. *Environ Pollut* 209:87–98
- Longhin E, Gualtieri M, Capasso L et al (2016b) Physico-chemical properties and biological effects of diesel and biomass particles. *Environ Pollut* 215:1–10. <https://doi.org/10.1016/j.envpo.2016.05.015>
- Luanpitpong S, Chen M, Knuckles T et al (2014) Appalachian mountaintop mining particulate matter induces neoplastic transformation of human bronchial epithelial cells and promotes tumor formation. *Environ Sci Technol* 48:12912–12919
- Mantecca P, Gualtieri M, Longhin E et al (2012) Adverse biological effects of Milan urban PM looking for suitable molecular markers of exposure. *Chem Ind Chem Eng Q* 18:635–641. <https://doi.org/10.2298/CICEQ120206114M>
- Melo S, Figueiredo J, Fernandes M et al (2017) Predicting the Functional Impact of CDH1 Missense Mutations in Hereditary Diffuse Gastric Cancer. *Int J Mol Sci* 18:2687. <https://doi.org/10.3390/ijms18122687>
- Ramirez RD, Sheridan S, Girard L et al (2004) immortalization of human bronchial epithelial cells in the absence of viral oncoproteins. *Cancer Res* 64:9027–9034
- Ramnefjell M, Aamelfot C, Helgeland L, Akslen LA (2017) Low expression of SerpinB2 is associated with reduced survival in lung adenocarcinomas. *Oncotarget* 8:90706–90718. <https://doi.org/10.18632/oncotarget.21456>
- Schaeffer D, Somarelli JA, Hanna G et al (2014) Cellular migration and invasion uncoupled: increased migration is not an inexorable consequence of epithelial-to-mesenchymal transition. *Mol Cell Biol* 34:3486–3499. <https://doi.org/10.1128/MCB.00694-14>
- Schroder WA, Major LD, Le TT et al (2014) Tumor cell-expressed SerpinB2 is present on microparticles and inhibits metastasis. *Cancer Med* 3:500–513
- Tseng C-Y, Chang J-F, Wang J-S et al (2015) Protective effects of *N*-acetyl cysteine against diesel exhaust particles-induced intracellular ROS generates pro-inflammatory cytokines to mediate the vascular permeability of capillary-like endothelial tubes. *PLoS One* 10:e0131911. <https://doi.org/10.1371/journal.pone.0131911>
- Valavanidis A, Vlachogianni T, Fiotakis K, Loridas S (2013) Pulmonary oxidative stress, inflammation and cancer: respirable particulate matter, fibrous dusts and ozone as major causes of lung carcinogenesis through reactive oxygen species mechanisms. *Int J Environ Res Public Health* 10:3886–3907. <https://doi.org/10.3390/ijerph10093886>
- Wei H, Liang F, Cheng W et al (2017) The mechanisms for lung cancer risk of PM_{2.5}: induction of epithelial-mesenchymal transition and cancer stem cell properties in human non-small cell lung cancer cells. *Environ Toxicol* 32:2341–2351. <https://doi.org/10.1002/tox.22437>
- Wu C, Zhu W, Qian J et al (2013) WT1 promotes invasion of NSCLC via suppression of CDH1. *J Thorac Oncol* 8:1163–1169. <https://doi.org/10.1097/JTO.0b013e31829f6a5f>
- Xiao D, He J (2010a) Epithelial mesenchymal transition and lung cancer. *J Thorac Dis* 2:154–159. <https://doi.org/10.3978/j.issn.2072-1439.2010.02.03.7>
- Xiao D, He J (2010b) Epithelial mesenchymal transition and lung cancer. *J Thorac Dis* 2:154–159
- Yang D, Ma M, Zhou W et al (2017) Inhibition of miR-32 activity promoted EMT induced by PM_{2.5} exposure through the modulation of the Smad1-mediated signaling pathways in lung cancer cells. *Chemosphere* 184:289–298. <https://doi.org/10.1016/j.chemosphere.2017.05.152>
- Yue H, Yun Y, Gao R, Li G, Sang N (2015) Winter polycyclic aromatic hydrocarbon-bound particulate matter from Peri-urban North China promotes lung cancer cell Metastasis. *Environ Sci Technol* 49(24):14484–14493. <https://doi.org/10.1021/es506280c>
- Zhang S, Zou L, Yang T et al (2015) The sGC activator inhibits the proliferation and migration, promotes the apoptosis of human pulmonary arterial smooth muscle cells via the up regulation of plasminogen activator inhibitor-2. *Exp Cell Res* 332:278–287. <https://doi.org/10.1016/j.yexcr.2015.02.006>